Performance Enhancement of Multi-Area Interconnected Power System using Revolutionary Energy Balance Control

B. Prakash Ayyappan*. Dr. R. Kanimozhi.**

**Assistant Professor, Department of Electrical and Electronics Engineering,*
V.S.B Engineering College, Karur, Tamilnadu, India. 639 111.
(e-mail: prakashayyappan78@gmail.com)
***Assistant Professor, Department of Electrical and Electronics Engineering,*
University College of Engineering, Anna University-BIT Campus, Tiruchirappalli, Tamilnadu, India.620 024.
(e-mail: kanimozhi_17@aubit.edu.in)

Abstract: In the current situation of the power system, with the need to increase power to meet the availability of all types of loads, the quality of power is equal to the demand. On this day, there is no change, and a demanding power supply with a stable and reliable power supply at all times. Therefore, in order to maintain the quality and power to meet the current reforms in the energy sector and to adapt to the changes in the demands of the industrial sector thus changing in frequency, an advanced controller is necessary. This work presents a Revolutionary Energy Balance Control (REBC) controller approach for Automatic Generation Controller (AGC). This AGC method focuses on balancing the whole generating system while maintaining a consistent system frequency per tie-lie power flow, with no load changes or power losses. In a Multi-Area Interconnected Power System (MIPS), a sudden load fluctuation, on the other hand, causes non-linearity (frequency deviation and tie-line) in all control regions. To lower the maximum deviation and oscillation duration, modelling error is taken into consideration. The main objective of FP-PID-based AGC is to preserve power system stability and reliability. The proposed technique is compared to standard two-area and three-area systems using data acquired in Simulink/MATLAB. The results show that the proposed technique has high dynamic responsiveness, economical operation, low magnitude error, and low frequency transients in MIPS. The performance of the REBC controller will be evaluated using metrics such as settling time, steady-state error, THD, and efficiency.

Keywords**: Multi-Area Interconnected Power System, frequency control, Revolutionary Energy Balance Control.**

1. INTRODUCTION

In order to run a reliable and stable electrical power system, a system frequency should be kept at a specified value or its deviation should be adjusted as quickly as possible in the event of load supply or demand changes. In a steady-state condition, a power system's whole capacity is used to supply loads. A sudden and abrupt shift in the load demand causes a mismatch between the load and the generated power. The MIPS power demand varies as a result of this circumstance. As a result, a control system is required to eliminate the mismatch problem by lowering the frequency and amount of tie-line power failures. To address these issues, this system proposed a sophisticated controller that combines a traditional PID controller with an adaptive controller known as the REBC controller. These methods are simple to use, provide quicker convergence, and only require a few parameters to correctly set up AGC development. This work employs the suggested REBC controller to provide good frequency regulation, estimate weighted load power, and investigate the nonlinear feature in error signals in multi-area, multi-source (thermal, PV, wind, and hydro) controlled power systems. A considerable Frequency Deviation (FD) is maintained under control because the REBC controller controls the flow of power in the tie-line from one location to another. A power analysis between unregulated load and power load violation is done to demonstrate the best of the proposed controller. The suggested approach has been proved to be better in terms of settling time (sec), steady-state error (%), THD (%), and efficiency (%).Finally, compare the performance of the proposed technique to that of existing state-of-the-art approaches. For the improvements of Multi-Source and Multi-Area system for stability in the proposed system, it needs to identify the drawback in the conventional methods that are given below. The Load Frequency Control is a fundamental mechanism in the interconnected power system. To deliver high-quality, reliable, and stable electrical power, the designed controller must function efficiently, that is, it must suppress regional frequency and tie-line power deviations. In this work, the LFC issue in multi-area power systems is solved using the Higher-Order Differential Feedback Controller (HODFC) and a created Fractional Order Differential Feedback Controller (FHODFC) [1]. A Virtual Generation Ecosystem Control (VGEC) approach that uses the time tunnel concept and the concept of new criteria to accomplish rapid automatic generation control power dispatch and optimum micro grid coordination[2-4]. This system presents the first theoretical stability analysis of AGC in a nonlinear power system that is interconnected. This Analysis is focused on singular perturbation theory, and it provides theoretical support for the widely held idea that AGC aids in the stabilization of systems operating on normal timescales [5-7]. The Area Control Error (ACE), also known as the Area Injection Error (AIE), involves direct monitoring of generator power levels in the condition of bias uncertainty and nonlinearity in generator turbine-governor reactions, this results in improved AGC performance [8-11]. A Dynamic Regulation Market Mechanism (DRMM) is presented in this system, which allows Demand Response (DR) units and generators to compete for regulation service in real time, assuring optimal allocation and lowering regulation service costs. [12-15]. When variable wind power is incorporated into power systems, the desired response may not be obtained. This work presented a Dynamic Gain Tuning Control (DGTC) technique for AGC to overcome these PQ issues [16-17]. This methodology is for evaluating the influence of various types of faults in the measurements used by the AGC system on power system dynamic performance. The statistics of system state variables are evaluated using stochastic system analysis approaches to address the random character of these errors. The convergence properties of these statistics are used to discover errors that cause instability [18-22]. Multi-area AGC's primary responsibilities include coordinating power exchange throughout subareas as well as maintaining power balance. By accomplishing cooperation among the participating generators, which are situated in different subarea networks that are interconnected, the newly established new power flow model enables multi-area AGC. [23-26].

2. MULTI SOURCE SYSTEM

The objectives of this work is to employ AGC to keep a nominal FD and tie-line power flow for MIPS. Maintaining a constant frequency with the speed governor is challenging for the MIPS system, thus it must be controlled to provide high-quality power in tie-line. As a result, an unique control mechanism has been developed to balance the effect of dynamic load fluctuations while maintaining a nominal frequency. Overall, the controller structure and accurate controller REBC control algorithm are obviously dependent on the optimal performance of the Power Supply System to decrease power loss and Frequency variation in the MIPS. In multi-area AGC, the REBC controller is used. There are four types of power plants in each area: thermal, wind, solar, and hydroelectric. This controller ensures that the power system runs smoothly and consistently. The suggested technique's performance is compared to that of many types of current controllers in two and three locations. The proposed technique is competitively superior, resilient, and stable in the event of a change in system features and random load disturbance. Based on this analysis, the proposed approach reduces the ACE errors' settling time per frequency and the oscillation of the current flow on the tie-line at each location. As a result, the suggested AGC controller might be used in real-time power supply system operation.

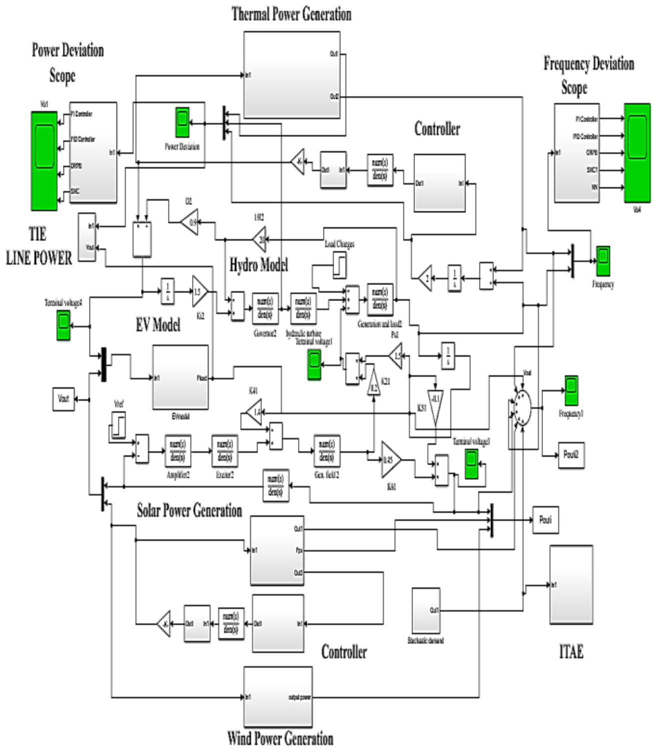

Fig. 1. Power system model of three-area with multi-source

2.1 Solar power generation

To generate the appropriate Voltage (V) and current (I), using a solar power system consists of many series and parallel coupled solar cell. The connection between V and I is non-linear due to that Solar radiation and load current influence the maximum power output of a PV array. As a result, a control strategy is necessary to obtain the greatest power from solar radiation. A PV system's output power may be stated as;

$$P_{EPV} = \eta S\varphi[1 - 0.005(T_a + 30) \quad (1)$$

Where T_a represents the ambient temperature (℃), S represents the PV array's measured area (m^2), S represents solar irradiation (kW/m^2), and S represents the PV array's conversion efficiency (%).The transfer function of a solar system may be calculated using a simple linear first-order lag equation (4).

$$G_{PV}(S) = \frac{\Delta P_{PV}}{\Delta\varphi} = \frac{K_{PV}}{1+sT_{PV}} \quad (2)$$

Where K_{PV} is gain constant and T_{PV} is a time constant.

2.2 Wind Generator (WG)

The air density and wind speed control the amount of electricity generated by wind power facilities. Where equation (3) shows how these two parameters influence the amount of power generated.

$$P_{WIND} = \frac{1}{2}.\alpha b.\rho.\beta i.V^3 \quad (3)$$

Where αb =Sweep area of blade inm^2, ρ = air density, βi = power co-efficient of air.

The following is an example of the WG transfer function model:

$$G_{Wind}(S) = \frac{\Delta P_{Wind}}{P_{Win}} = \frac{K_{WTG}}{1+s.T_{WTG}} \quad (4)$$

K_{WTG}=wind turbine gain,
T_{WTG} =Time based turbine gain

2.3 Thermal Generator

The thermal generator model in the LFC research has four components. The transfer functions of generators, steam turbines, governors, and re-heaters are among these components. Figure 2 illustrates the heat generator's transfer function model, which includes all components.

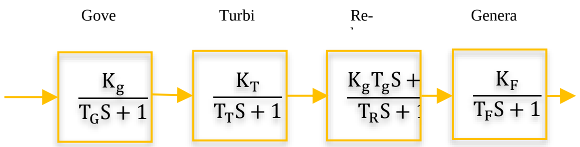

Fig. 2. Transfer function model of the thermal generator

The Frequency regulation is improved by two control loops in the heat-generating structure. The heat-generating unit assists in the frequency adjustment of the governor from the first cycle. Even if the first cycle is useful for detecting large frequency fluctuations, the constant-level inaccuracy in the frequency signal is a major concern in the implementation of this control loop. As a result, Area Control Error (ACE) supplemental loop signals can be used to reduce static error. The ACE signal is expressed mathematically as follows:

$$ACE_i = \Delta P_{tie,i} + \beta_i \Delta f_i \quad (5)$$

The regional bias factors of the network connection, tie-line power, and FD of the i-th area, respectively, are β_I,$\Delta P_{tie,i}$andΔf_I in this study. The heat generator's basic construction contains two frequency control loops, which will be discussed in the next section.

2.4 Hydropower generation

The main mover slows to compensate for the power imbalance, but the power generation controls the speed. As the speed change decreases, the error signal lowers, and the governor speed becomes constant. Because the load changes over time, it is difficult to set the governor speed to a fixed value; hence, this system employs a control system with an integrator. To eliminate offsets, the control system analyses the change and adapts as needed. A system's reset point refers to its capacity to return to its starting state. As a result, the AGC is a frequency-adjustment mechanism that does so automatically. The AGC for a given site is depicted in Figure 3. The AGC is made up of a governor device that sends a signal to the turbine to change its speed in order to maintain a consistent frequency.

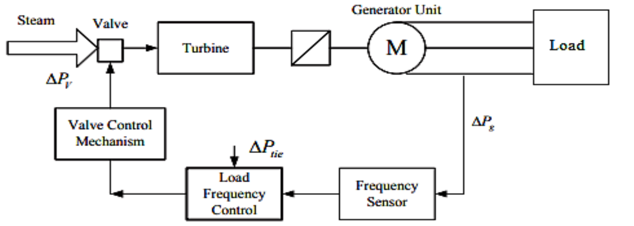

Fig. 3. Functional block for the thermal generator

The system's three most important components are the governor, prime mover load, and inertia model. The system's block diagram, represented in Figure 4, may be expressed using equations (6 to 8). The following is a list of them:

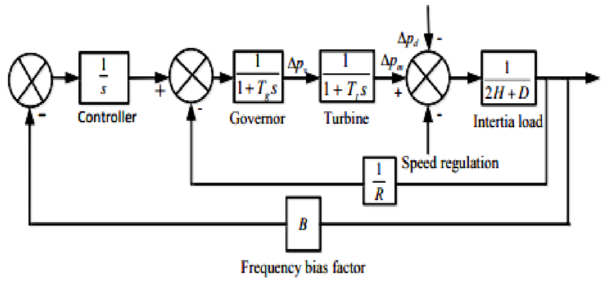

Fig. 4. Control block diagram for the thermal generation Governor model

The hydraulic amplifier converts the command ΔP_g to the position of the steam valveΔP_V . $T_g$is the governor's time constant, and the equation 6 is the governor's transfer function. 6

$$\frac{\Delta P_V(s)}{\Delta P_g(s)} = \frac{1}{1+T_g s} \quad (6)$$

Prime mover model: The speed load characteristic equation may be used to examine the motor load, which is sensitive to frequency changes. As indicated in equation (7), the prime mover model, ΔP_m couples the mechanical power output to the change in the ΔP_V steam valve.

$$\frac{\Delta P_m(s)}{\Delta P_V(s)} = \frac{1}{1+T_t s} \quad (7)$$

Load and inertia model: The speed load characteristic equation may be used to examine the motor load, which is sensitive to frequency changes. (8).

$$\frac{\Delta P_m(s)}{\Delta P_m - \Delta P_l} = \frac{1}{2H+D} \quad (8)$$

Frequency bias factor: As mentioned in equation, (9) the frequency biased factor is the sum of frequency-sensitive load change (D) and speed regulation (9).

$$B = \frac{1}{R} + D \quad (9)$$

2.5 Design of Revolutionary Energy Balance Control Algorithm controllers

In this work, a novel Revolutionary Energy Balance Control Algorithm (REBC) controller is implemented as a FOPID controller to change the parameters of a multi-area power system. In comparison to conventional controllers, fractional-order controllers offer additional tuning options, higher responsiveness with high order, and non-minimum phase systems. The integral portion, on the other hand, enhances the steady-state response in a normal Proportional Integral Derivative (PID) controller. On the other aspect, it causes system response to be delayed and diminishes relative stability. The derivative element enhances dynamic responsiveness, speeds up the system, and increases stability. Furthermore, it increases the system's sensitivity to noise disruptions. In this system utilize a fractional-order controller to balance the advantages and disadvantages of a standard PID controller. The fractional integral/derivative portion was used instead of the pure integral ($\frac{1}{s}$) derivative (s) part in this work. The proposed FOPID-based REBC controller is represented in Figure 5 as a block diagram. The FOPID-based REBC controller's input signal is f, and its output "y" is transmitted to the next stage controller, the (1+PI) controller, to generate the presented FOPID-(1+PI) controller's final response, as shown in Figure 5. In addition to the FOPID control signals, the controller described here is also available (10, 11).

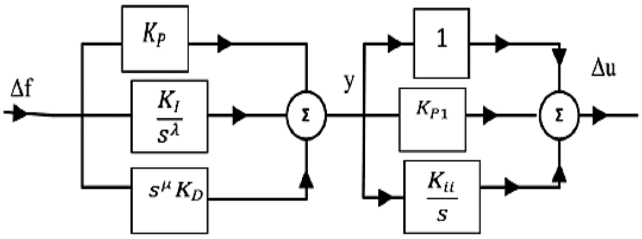

Fig. 5. Block diagram for the FOPID based REBC controller

$$Y = K_P\Delta f + K_{Is^{-\lambda}}\Delta F + K_P s\mu\Delta f \quad (10)$$

$$\Delta u = \left[(K_P\Delta f + K_{Is^{-\lambda}}\Delta F + K_P s\mu\Delta f)\right] \times [(1 + K_{P1} + K_{iiS^{-1}}] \quad (11)$$

In simulation or other practical applications, the integer order transfer function is necessary to generate fractional-order differentiators or integrators. Infinite-dimension fractional-order differentiators or integrators in the relevant frequency range must be approximated in order to do so. This is evaluated using time-domain rational approximation methods and sub-optimal approximation methodologies. The transfer function of a filter in the considered frequency range (ω_b, ω_h) is (12).

$$G_{rationalfilter(S)} = K\pi_{K=-N}^{N}\left(\frac{S+W_1'}{S+W_1}\right) \quad (12)$$

The rational filter's zeros, poles, and gain are provided by (13), (14), and (15), respectively.

$$W_1' = W_b\left(\frac{W_h}{W_b}\right)^{\frac{1+N+\frac{(1-\beta)}{2}}{2N+1}} \quad (13)$$

$$W_1 = W_b\left(\frac{W_h}{W_b}\right)^{\frac{1+N+\frac{(1-\beta)}{2}}{2N+1}} \quad (14)$$

$$K=W_h^{\beta} \quad (15)$$

The integrator/order differentiator's is "2N+1," whereas β the filter's order is "2N+1." For all fractional-order elements, the fifth-order time-domain approximation in the frequency region of 0.01, 100 radian per sec has been addressed. The Load Frequency (LF) is reduced by utilizing a low-order approximation, but the amplitude and phase responses of ripple production are increased.

2.6 Proposed system Revolutionary Energy Balance Control Algorithm

The determination of sudden and random variation has a direct effect on the system dynamics and is just as significant as the optimization approach's performance. Sudden and random variation should be used to achieve goals like rapid and non-oscillated system response with low overshoot and steady-state inaccuracy. The use of Revolutionary Energy Balance Control (REBC) in control engineering allows for more accurate system modelling or control system design, as well as greater robustness and adaptability. The Revolutionary Energy Balance Control (REBC) algorithm's steps are described below.

2.6.1 REBC Algorithm Steps

Step1: Initialization of devices.
Step2: Initially, the source power is turned on.
Step3: Define the objective function in which the design variables are constrained equally and unequally.
Step 4: Set the population size to the iteration number, and the design variables to the DG and location sizes.
Step 5: Determine the value of the goal function using the forward-backward load flow.

$$F(\times) = \min \sum_{I=1}^{b} R_1 * I_1^2 \quad (16)$$

Step 6: Set the number of iterations to 1 and look for the best population/learner with the best objective function value. Calculate the population's mean as well.
Step 7: Update the previous solutions with the following statement, then go on to all acceptable solutions that are better than current teacher's.

$$D\_M_{s,k} = r_K(\times_{s,kbest,k} - T_D M_{s,k}) \quad (17)$$

In the subject "s," is the best learner's (or teacher's) outcome TD is the Training Quality Factor, which is the root reason for enhancing or modifying the mean class result in that subject $\times_{s,kbest,k}$ is a uniformly distributed random integer between [0, 1], and TD is the Training Quality Factor, which is the root reason for enhancing or modifying the mean class result in that subject Ms,k. The Fractional Order Controller (FOC) can be either 1 or 2, and it is selected at random with equal probability as shown in Equation.
Step 8: Using the Equation below, modify the solutions obtained in step 5 and carry forward any acceptable options that result in a better solution than the current position.

$$X_{i,s,k}' = X_{i,s,k}' + DM_{s,k} \quad (18)$$

All updated $X'_{i,s,k}$ values generate a better function value, they are used as input for the next cycle/iteration; otherwise, they are left unchanged.

Step 9: Repeat steps 6–8 until the total number of iterations reaches the maximum number of iterations.

Step 10: Finally, represent the best solution/teacher as the best solution, plot the best position records from all iterations as convergence characteristics, and then stop.

3. RESULT AND DISCUSSION

The research work based on AC frequency regulation in grid-connected Multi Area-Multi Source (MAMS) power generation has progressed due to an improved version of MATLAB/Simulink software. Renewable energy power production has proposed a transfer function model in the Simulink environment based on the MAMS system, and it has been suggested that the program development required for optimization technology is built in the 2017 b MATLAB software environment M file. This section increases the efficacy of a number of proposed methods in MIPS systems in response to AC frequency stabilization. The proposed model's analysis has progressed with various evaluations such as (i) Frequency stabilization in MAMS system (ii) controller performance under dynamic test condition (iii) steady-state analysis (%)(iv) Settling time (sec)Overshoot (%), Integral Time Absolute Error(ITAE) (%), and efficiency (%).The performance of interconnected power systems is evaluated under various load circumstances in this MSSA ((20%, 50%, and 100 %). Performance measures such as steady-state error (%), settling time (sec), Overshoot (%), Integral Time Absolute Error (ITAE), and efficiency (%) are examined using various control methodologies based on the test data. The results of the various load condition-based tests are shown in the figures and tabulations below.

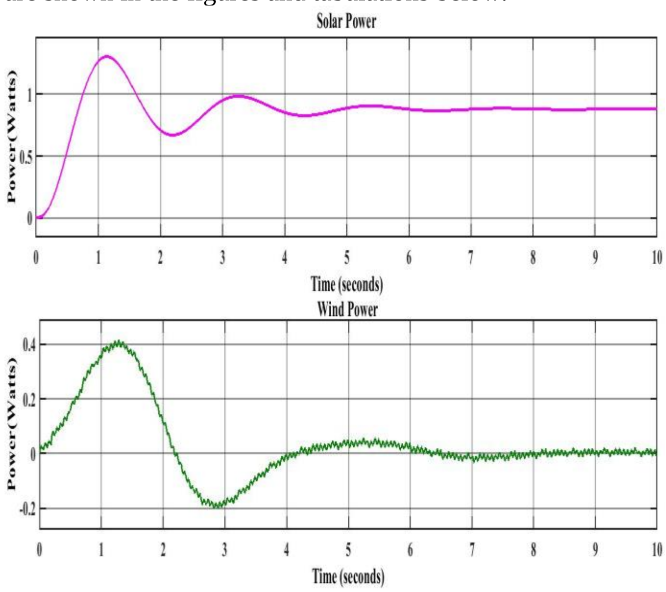

Fig. 7. Solar and wind generation waveform

Figure 7 illustrates solar and wind energy generation; the above waveform clearly depicts power generation throughout various periods. Feedback is delivered to the FOPID in order to sustain both the solar and wind generating singles fluctuations. An automated generation control is offered as a result of this procedure, and the generated power is regulated. The energy deviation of the solar and wind generation systems is analyzed based on the load system's operating state, as shown in the figures (10, 15, and 20).

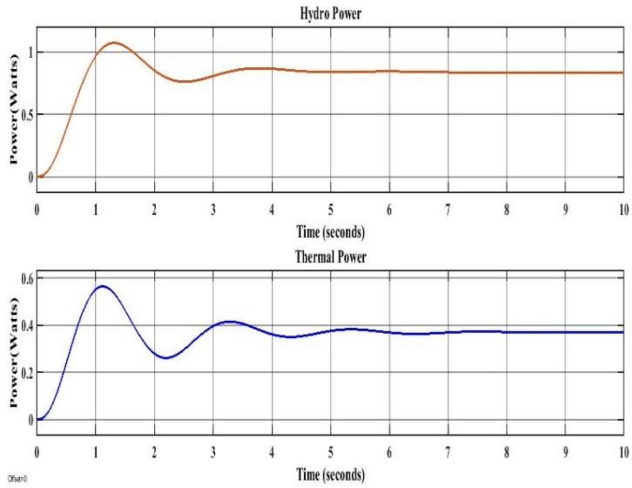

Fig. 8. Thermal-hydro Power Generation Waveform

Figure 8 represents multi-power generating waveforms, also known as thermal and hydro power-producing waveforms. All of the power-producing facilities are used as auxiliary power sources in the MIPS, which successfully balances the grid power line under dynamic load fluctuation scenarios. The proposed REBC based converter system continually provides energy for the bus system due to the thermal and hydropower producing systems. As shown below, the performance of the MSSA connected power system was examined under various load circumstances, including 20%, 50%, and 100%.

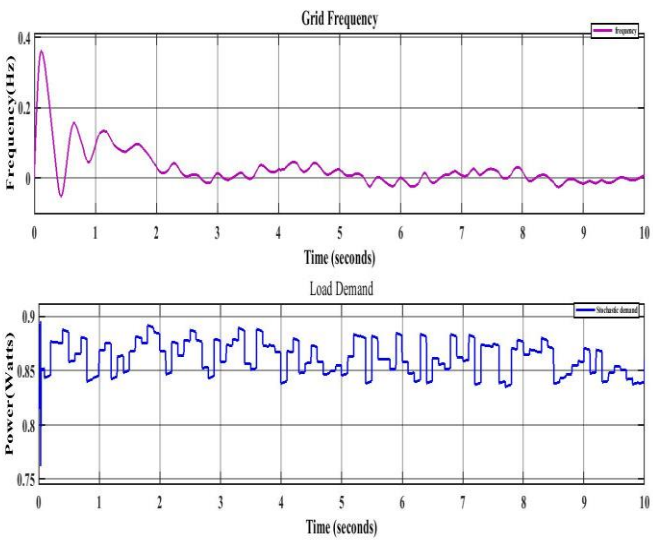

Fig. 9. Grid frequency with 20% load varying system

Figure 9 shows the suggested grid frequency analysis, which is based on the REBC algorithm, and is tested with various stochastic load demands. The system's dynamic load fluctuation will create higher frequency variation, however, the suggested REBC would produce reduced frequency variation during 20 percent load circumstances, as illustrated in figure 10.

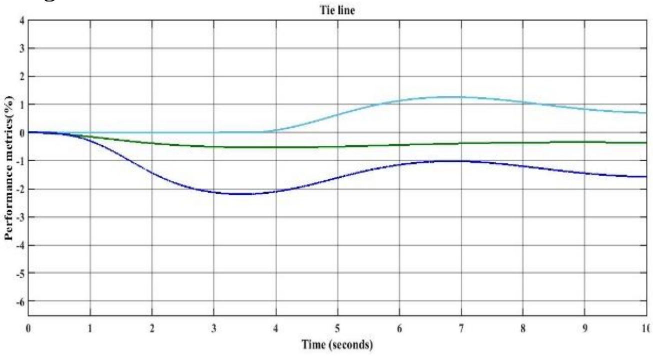

Fig. 10. Tie Line power stability analysis

Figure 11 shows the tie-line power stability investigation of the recommended multi-source-single area interconnected model under dynamic load shifting conditions. When comparing several controllers such as the PI, PID, and REBC controllers, the REBC controller produces a better result.

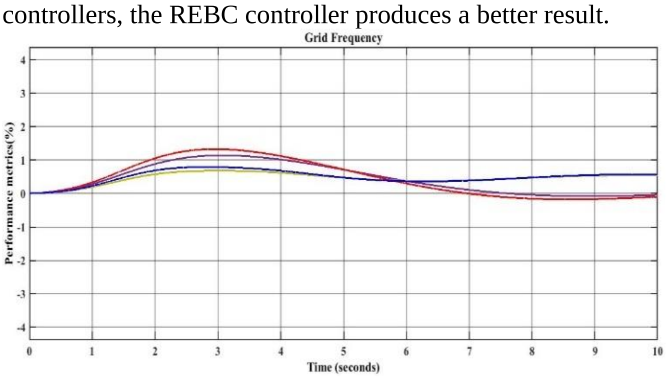

Fig. 11. Grid frequency based on different control approaches

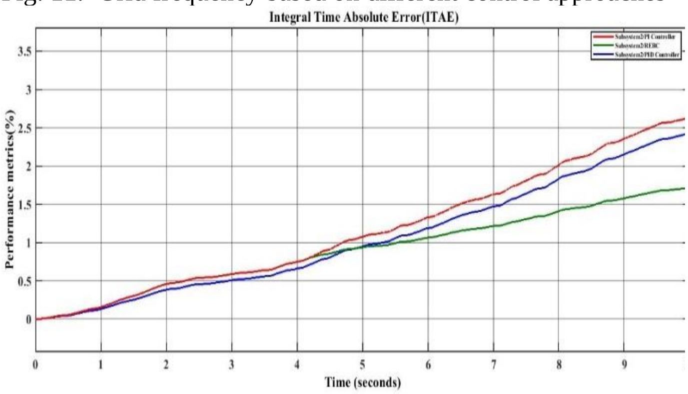

Fig. 12. ITAE using different control technique

The outcome of Integral Time Absolute Error (ITAE) employing various control approaches is shown in Figure 12. REBC calculates a 1.46% error ratio based on this ITAE analysis.

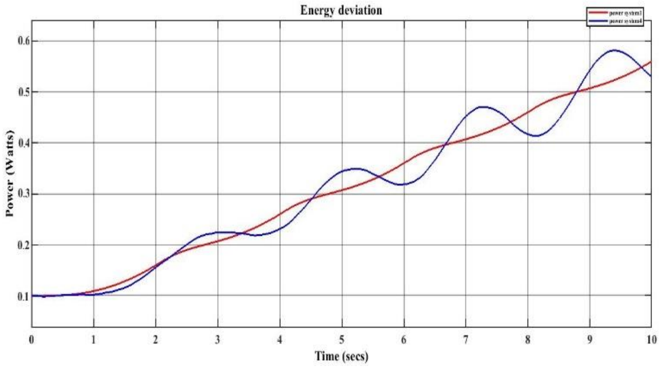

Fig. 13. Energy deviation using different control techniques

The maximum amount of load change for the MIPS is shown in Figure 13. The suggested REBC controller performs better in both power system 1 (solar) and power system 2 (wind) energy sources under 20 percent load-changing situations.

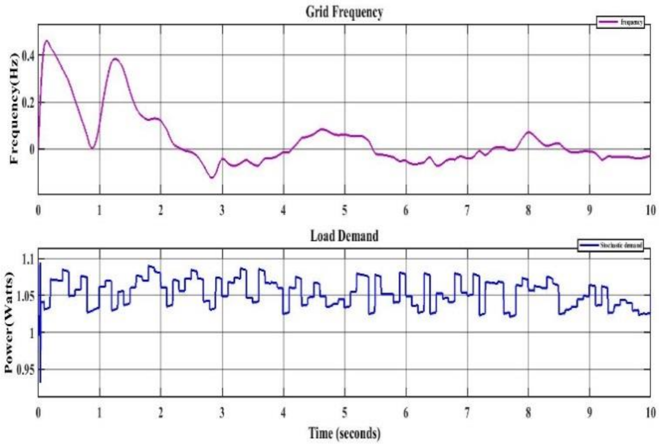

Fig. 14. Grid frequency with 50% load varying system

Figure 14 illustrates the suggested grid frequency survey, which is based on the REBC algorithm and tested with various stochastic load demands.

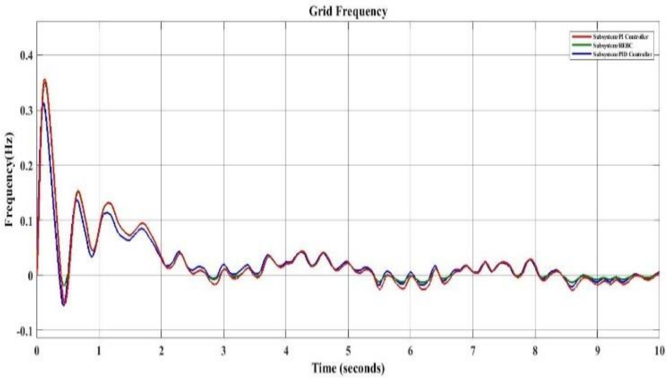

Fig.15. Grid frequency based on different control approaches

The system's dynamic load shift will create higher frequency fluctuation, however, the suggested REBC would provide reduced frequency variation during 50 percent load circumstances, as illustrated in figure 15.

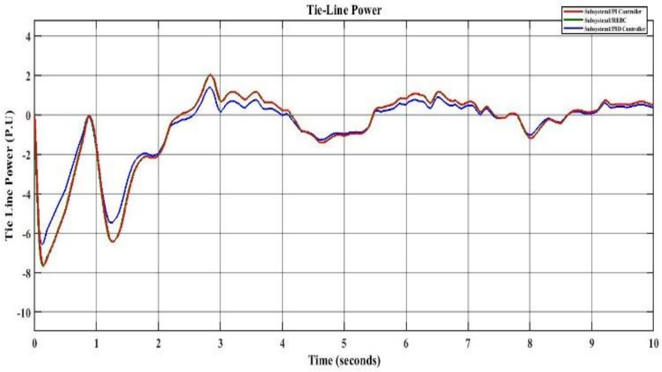

Fig. 16. Tie Line power stability analysis for 50% load system

Figure 16 represents the suggested multi-source-single-area interconnected model's tie-line power stability study for 50 percent load changing circumstances. In a comparison of several controllers, the REBC controller outperforms the PI, PID, and REBC controllers under 50 percent load-changing situations.

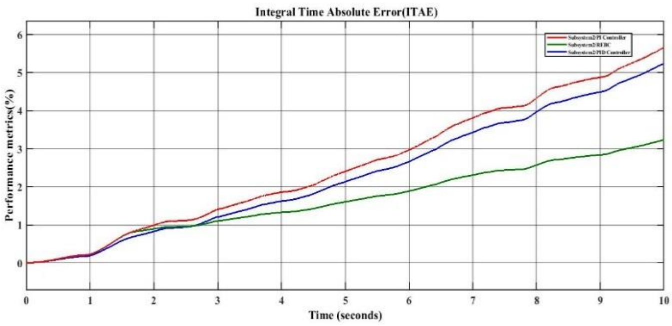

Fig. 17. ITAE using different control technique

Figure 17 shows Integral Time Absolute Error (ITAE) using various control methodologies under 50 percent load fluctuation circumstances. Based on this ITAE analysis, REBC calculates a 2.0 percent error ratio.

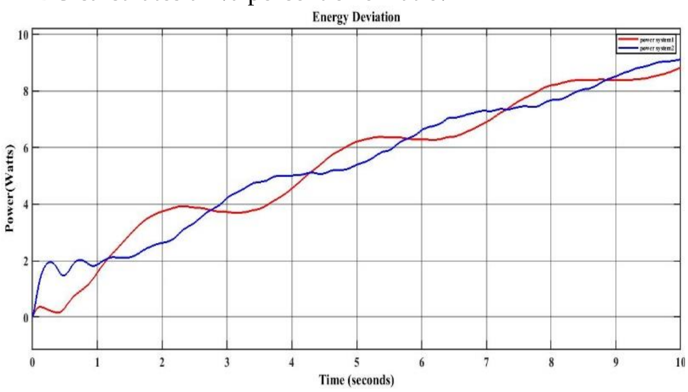

Fig. 18. Energy deviation using different control techniques

The maximum amount of load change for the MSSA Interconnected Power System is shown in Figure 18. Variable conditions are studied for 50 percent load; the suggested REBC controller performs better in power system 1 (solar) and power system 2 (wind) energy sources.

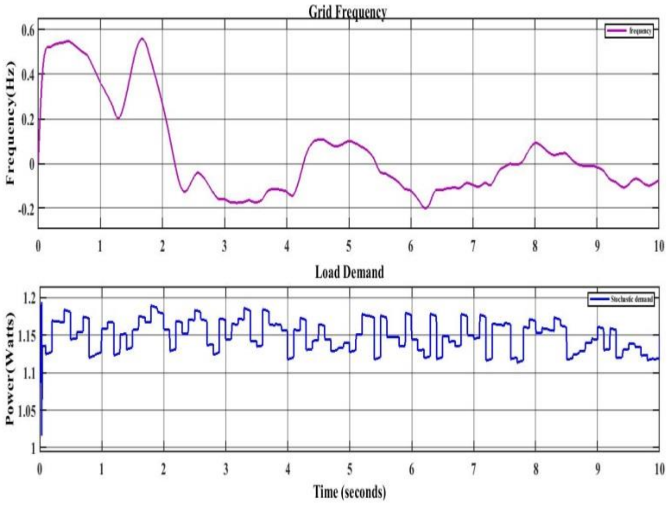

Fig. 19. Grid frequency with 100% load varying system

Figure 19 demonstrates a suggested grid frequency survey based on the REBC algorithm, with several stochastic 100 percent load demand situations being examined.

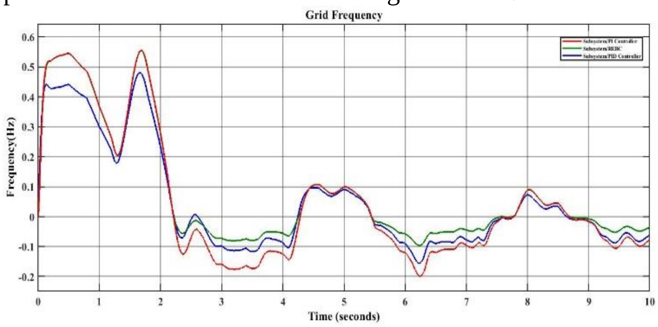

Fig. 20. Grid frequency based on different control approaches

The system's dynamic load fluctuation will create higher frequency variation, however, the suggested REBC would provide reduced frequency variation during 100% load circumstances, as illustrated in figure 20.

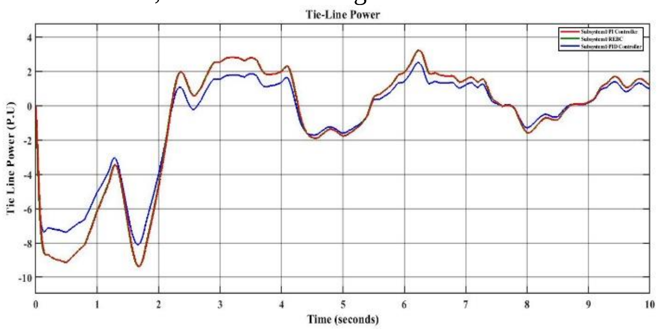

Fig. 21. Tie Line power stability analysis for 100% load system

The suggested multi source-single area interconnected model's tie-line power stability analysis under 100 percent load changing situations is shown in Figure 22. The PI, PID, and REBC controllers were shown to be the most effective when compared to other controllers. Under 50 percent load varying situations, the REBC performs well.

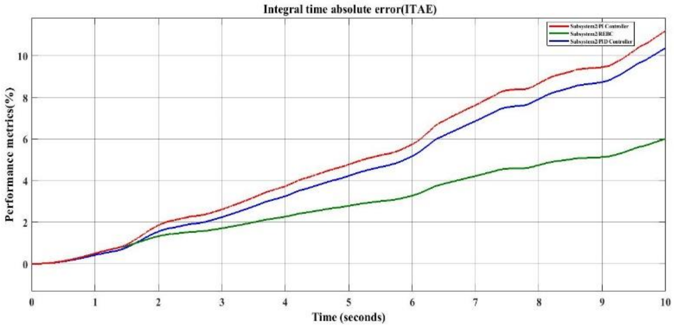

Fig. 22. ITAE using different control technique

Figure 22 illustrates the Integral Time Absolute Error (ITAE) employing various control strategies in a system with a 100% load variation. REBC calculates a 4.0 percent error ratio based on this ITAE analysis.

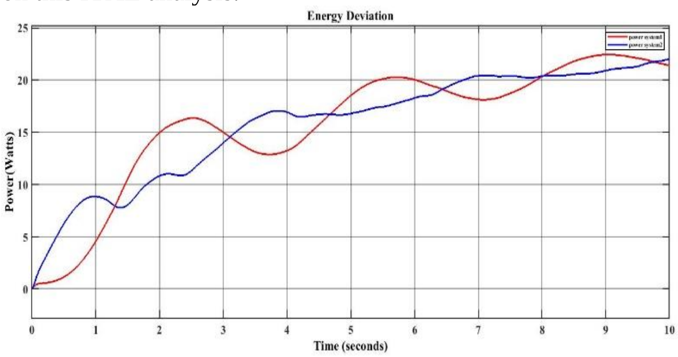

Fig. 23. Energy deviation using different control techniques

The maximum amount of load change for the MSSA Interconnected Power System is shown in Figure 23. Dynamic conditions are examined for 100 percent load; the suggested REBC controller performs better in power system 1 (solar) and power system 2 (wind) energy sources.

Table 1 Performance analysis of the proposed model based on different aspects

Variations	Parameters	PI controller	PID Controller	REBC controller
Power system-1	Settling Time(sec)	0.59	0.47	0.37
	Peak Overshoot (%)	0.089	0.069	0.039
	Steady-state error (%)	0.6.9	0.58	0.39
Power system-2	Settling Time(sec)	0.55	0.39	0.34
	Peak Overshoot (%)	0.071	0.064	0.033
	Steady-state error (%)	0.64	0.48	0.35
Tie Line	Settling Time(sec)	0.52	0.40	0.34
	Peak Overshoot (%)	0.070	0.058	0.032
	Steady-state error (%)	0.60	0.45	0.31

The suggested Area-based Performance Analysis of the proposed model is shown in Table 1. The suggested model gives an effective outcome based on the aforementioned parameters, settling time (sec), Peak Overshoot (%), and Steady-state error (%).

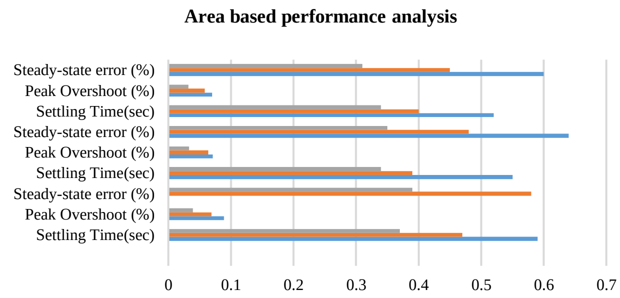

		Settling Time(sec)	Peak Overshoot (%)	Steady-state error (%)	Settling Time(sec)	Peak Overshoot (%)	Steady-state error (%)	Settling Time(sec)	Peak Overshoot (%)	Steady-state error (%)
REBC	0	0.37	0.039	0.39	0.34	0.033	0.35	0.34	0.032	0.31
PID	0	0.47	0.069	0.58	0.39	0.064	0.48	0.4	0.058	0.45
PI	0	0.59	0.089	0	0.55	0.071	0.64	0.52	0.07	0.6

REBC PID PI

Fig. 24. comparison analysis based on the different areas of the interconnected system

The comparative examination of the several source locations of the linked system is shown in Figure 24. The performance of the power system-1, power system-2, and the tie-line system is evaluated using several criteria such as Settling Time (sec), Peak Overshoot (%), and Steady-state Error (%).

Table 2 Performance analysis of the proposed model with and without the controller

Variations	Parameters	Without REBC Controller	With REBC controller	% Improvement
Power system-1	Peak Time(sec)	0.70	0.35	30.21
	Peak Overshoot (%)	0.075	0.040	37.67
	settling time (sec)	0.70	0.44	27.36
Power system-2	Peak Time(sec)	0.70	0.36	34.65
	Peak Overshoot (%)	0.075	0.035	35.79
	Steady-state error (%)	0.65	0.38	29.64
Tie Line	Peak Time(sec)	0.70	0.35	30.16
	Peak Overshoot (%)	0.073	0.036	36.64
	settling time (sec)	0.63	0.34	30.33

The performance evaluation of the suggested model with and without the REBC controller is shown in Table 2. Based on the examination of several characteristics such as peak Time (sec), Peak Overshoot (%), and Steady-state error (%) the suggested REBC controller outperforms with and without controller model.

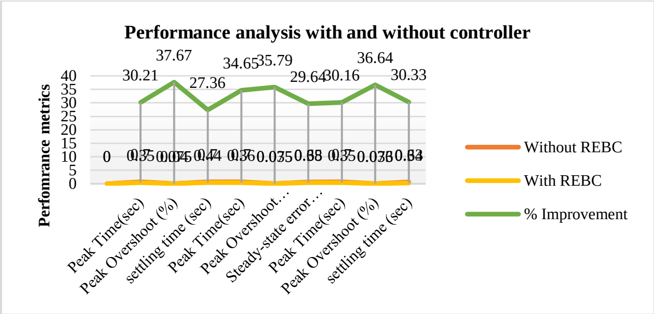

Fig. 25. comparative analysis based on with and without a controller

Figure 25 shows a comparison of the connected system's different source areas with and without the REBC controller. The proposed REBC controller outperforms both the controller model and the model without it, according to the findings of the previous work.

Table 3 system damping characteristics with the optimized controllers

System Oscillatory modes	∫	F(Hz)	ITAE	M_P	T_P	T_s
20% oscillatory mode	0.824	49.54	1.46	0.0441	3.754	0.3
50% oscillatory mode	0.604	49.61	2.0	0.0393	2.432	0.44
100% oscillatory mode	0.489	49.38	4.0	0.0453	3.31	0.52

The damping measures, such as the value of the ITAE index, the maximum peak value (M_P) , peak time (T_P), and settling time (T_s)Parameters are analysed with system oscillation mode (20%, 50%, and 100%), and damping Ratio (∫) relative to the proposed controller are determined in table 3.

Table 4. MSSA interconnected system Performance analysis function of proposed system using REBC and existing systems

Parameters	PI	PID	REBC
Steady-state error (%)	1.8	1.2	0.6
Settling time (sec)	0.46	0.38	0.29
Overshoot (%)	0.079	0.045	0.024
Integral Time Absolute Error (ITAE) (%)	0.0621	0.0458	0.026
Efficiency (%)	87.5	89.9	92.5

Table.4 represents the proposed MSSA interconnected system's performance analysis function using different control techniques like PI, PID, and the proposed REBC control systems; based on the analysis, the proposed REBC techniques produce a better result.

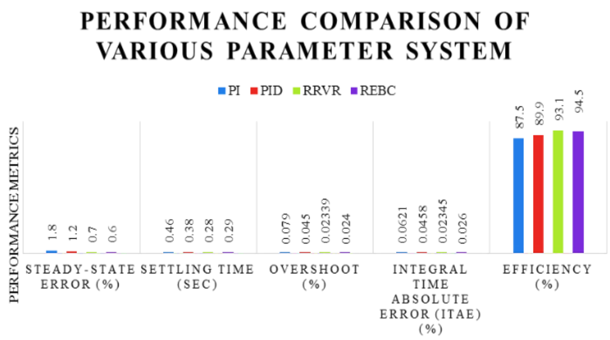

Fig. 26. Performance analysis of the MSSA interconnected system

Figure.26 illustrates a comparison of the MIPS system using different characteristics such as steady-state error (%), settling time (sec), overshoot (%), and Integral Time Absolute Error (ITAE). The suggested REBC may offer reliable results when compared to other current controllers, according to the effective comparison analysis.

4. CONCLUSION

In this work operating frequency is a critical performance indicator for power system stability and security. During nominal power system operation, the system's frequency should be within a very limited and acceptable interval around its nominal value. AGC controllers are widely used to modulate system frequency depending on control center actions in order to create an actual power balance between generation and load. Dynamic responses have been seen in a power system using a REBC adjusted AGC controller. The optimal gains of generation-based AGC controllers are determined by the scheduled load allocated by numerous sources of power generation. The proposed Revolutionary Energy Balance Control (REBC) controller techniques are assessed using a number of parameters, including steady-state error (0.6%) and system efficiency (94.5 %).

REFERENCES

Beyda Tasar, Hasan Giiler and mehmet Ozdemir, (2015). The Investigation of Fuzzy Logic-PI Based Load Frequency Control of Keban HEPP. *Control Engineering and Applied Informatics*, 4, 71-80.

Fakharian.A, Rahmani. R, (2016). An Optimal Controlling Approach for Voltage Regulation and Frequency Stabilization in Islanded Microgrid System, *Control Engineering and Applied Informatics*, 18, 107-114.

Vijayakumar. K, Manigandan. T, (2016), Nonlinear PID Controller Parameter Optimization using Enhanced Genetic Algorithm for Nonlinear Control System, *Control Engineering and Applied Informatics*, 18, 3-10.

Anbarasi. S and Muralidharan. S, (2016). Enhancing the Transient Performances and Stability of AVR System with BFOA Tuned PID Controller, *Control Engineering and Applied Informatics*, 18, 20-29.

Van Van Huynh, Hoang-Duy Vo, Bach Hoang Dinh, Thanh-Phuong Tran and Minh Hoang Quang Tran, (2018). A New Adaptive Second Order Sliding Mode Control Design for Complex Interconnected Systems, *Control Engineering and Applied Informatics*, 20, 3-14.

Sahin. E, (2020). Design of an Optimized Fractional High Order Differential Feedback Controller for Load Frequency Control of a Multi-Area Multi-Source Power System With Nonlinearity, *IEEE Access*, 8, 12327-12342.

Xi.L, (2020). A Virtual Generation Ecosystem Control Strategy for Automatic Generation Control of Interconnected Microgrids, *IEEE Access*, 8, 94165-94175.

Daraz. A, Malik. S.A, Mokhlis. H, Haq. I.U, G. F. Laghari and N. N. Mansor, (2020). Fitness Dependent Optimizer-Based Automatic Generation Control of Multi-Source Interconnected Power System With Non-Linearities, *IEEE Access*, 8, 100989-101003.

Qiu.Y, Lin. J, Liu. F and Song. Y, (2020). Explicit MPC Based on the Galerkin Method for AGC Considering Volatile Generations, *IEEE Transactions on Power Systems*, 35, 462-473.

Tan.C, (2020). Multi-Area Automatic Generation Control Scheme Considering Frequency Quality in Southwest China Grid: Challenges and Solutions, *IEEE Access*, 8, 199813-199828.

Simpson-Porco. J.W, (2021). On Area Control Errors, Area Injection Errors, and Textbook Automatic Generation Control, *IEEE Transactions on Power Systems*, 36, 557-560.

Daraz. A, Malik. S.A, Mokhlis. H, Haq. I.U, Zafar. F and Mansor. N.N, (2020). Improved-Fitness Dependent Optimizer Based FOI-PD Controller for Automatic Generation Control of Multi-Source Interconnected Power System in Deregulated Environment, *IEEE Access*, 8, 197757-197775.

Li.J and Yu.T, (2020). Deep Reinforcement Learning Based Multi-Objective Integrated Automatic Generation Control for Multiple Continuous Power Disturbances, *IEEE Access*, 8, 156839-156850.

Lackner. C, Osipov.D , Cui. H and Chow. J.H, (2020). A Privacy-Preserving Distributed Wide-Area Automatic Generation Control Scheme, *IEEE Access*, 8, 212699-212708.

Shiltz. D.J, Baros. S, Cvetković. M and Annaswamy. A.M, (2019). Integration of Automatic Generation Control and Demand Response via a Dynamic Regulation Market Mechanism, *IEEE Transactions on Control Systems Technology*, 27, 631-646.

Chen. X, Lin. J, Liu. F and Song. Y, (2019). Optimal Control of AGC Systems Considering Non-Gaussian Wind Power Uncertainty, *IEEE Transactions on Power Systems*, 34, 2730-2743.

Patel. R, Li. C, Meegahapola. L, McGrath. B and Yu. X, (2019). Enhancing Optimal Automatic Generation Control in a Multi-Area Power System with Diverse Energy Resources, *IEEE Transactions on Power Systems*, 34, 3465-3475.

Wang. H, Lei. Z, Zhang. X, Peng. J and Jiang. H, (2019). Multiobjective Reinforcement Learning-Based Intelligent Approach for Optimization of Activation Rules in Automatic Generation Control, *IEEE Access*, 7, 17480-17492.

Xu. Y, Li. F, Jin. Z and Hassani Variani. M, (2016). Dynamic Gain-Tuning Control (DGTC) Approach for AGC With Effects of Wind Power, *IEEE Transactions on Power Systems*, 31, 3339-3348.

Kammer. C and Karimi. A, (2019). Decentralized and Distributed Transient Control for Microgrids, *IEEE Transactions on Control Systems Technology*, 27, 311-322.

Zhang. J and Domínguez-García. A.D, (2018). On the Impact of Measurement Errors on Power System Automatic Generation Control, *IEEE Transactions on Smart Grid*, 9, 1859-1868.

Pathak. N, Bhatti. T.S, Verma. A and Nasiruddin. I, (2018). AGC of Two Area Power System Based on Different Power Output Control Strategies of Thermal Power Generation, *IEEE Transactions on Power Systems*, 33, 2040-2052.

Prostejovsky. A.M, Marinelli. M, Rezkalla. M, Syed. M.H and Guillo-Sansano. E, (2018). Tuningless Load Frequency Control Through Active Engagement of Distributed Resources, *IEEE Transactions on Power Systems*, 33, 2929-2939.

X. S. Zhang, T. Yu, Z. N. Pan, B. Yang and T. Bao, (2018). Lifelong Learning for Complementary Generation Control of Interconnected Power Grids With High-Penetration Renewables and EVs, *IEEE Transactions on Power Systems*, 33, 4097-4110.

D. Ganger, J. Zhang and V. Vittal, (2018). Forecast-Based Anticipatory Frequency Control in Power Systems, *IEEE Transactions on Power Systems*, 331004-1012.

X. Dong, (2017). Power Flow Analysis Considering Automatic Generation Control for Multi-Area Interconnection Power Networks, *IEEE Transactions on Industry Applications*, 53, 5200-5208.

Z. Li, C. Zang, P. Zeng, H. Yu and H. Li, (2016). MAS based distributed automatic generation control for cyber-physical microgrid system, *IEEE/CAA Journal of Automatica Sinica*, 3, 78-89.

D. Apostolopoulou, A. D. Domínguez-García and P. W. Sauer, (2016). An Assessment of the Impact of Uncertainty on Automatic Generation Control Systems, *IEEE Transactions on Power Systems*, 31, 2657-2665.

S. Liu, P. X. Liu and A. E. Saddik, (2015). Modeling and Stability Analysis of Automatic Generation Control Over Cognitive Radio Networks in Smart Grids, *IEEE Transactions on Systems, Man, and Cybernetics: Systems*, 45, 223-234.